Ecological Indicators 90 (2018) 569–576

Contents lists available at ScienceDirect

Ecological Indicators

journal homepage: www.elsevier.com/locate/ecolind

Original Articles

Prediction of effective climate change indicators using statistical downscaling approach and impact assessment on pearl millet (*Pennisetum glaucum* L.) yield through Genetic Algorithm in Punjab, Pakistan

Asmat Ullah[a,b,c,*], Nasrin Salehnia[c,d], Sohrab Kolsoumi[d], Ashfaq Ahmad[e], Tasneem Khaliq[a]

[a] Department of Agronomy, Agro Climatology Lab., University of Agriculture, Faisalabad 38040 Pakistan
[b] Agronomic Research Station, Karor-31100 Layyah, Punjab, Pakistan
[c] Institute for Sustainable Food Systems, University of Florida, 32611-0570, USA
[d] Ferdowsi University of Mashhad, P.O. Box: 9177-949207, Mashhad, Iran
[e] Program Chair, Climate Change, US-Pakistan Centre for Advanced Studies (A&FS), University of Agriculture Faisalabad, 38040, Pakistan

ARTICLE INFO

Keywords:
AgMERRA dataset
Agrometeorology
Delta method
Diurnal temperature
MIRCO5
Artificial intelligence method

ABSTRACT

Climate change involves long term changes in climate including increase in temperature, elevated CO_2 and uneven distribution of rainfall quantity and periodicity. Though daily mean temperature (T_{mean}) is considered a widely useful index of assessment of climate change, averaging can obscure some of the variations expected in diurnal temperature range (DTR). The aim of this study was to evaluate the effectiveness of DTR relative to T_{mean} as a metric for predicting millet yield using a combination of a historical dataset (1980–2010) and two climate model (MIROC5 and GFDL) projections for 2017–2046 under RCP 4.5 and 8.5 across two different environments (arid, Layyah and semi-arid, Faisalabad) of Punjab, Pakistan. Provincial datasets of pearl millet yields were collected and checked for an empirical relationship between T_{mean}, DTR and crop yield. The mean of projections showed increasing DTR relative to baseline in both environments. Projected T_{max} and T_{min} were highly correlated (0.90–0.99) for both environments and climate models. MIROC5 predicted T_{max} and T_{min} well and GFDL performed efficiently in predicting precipitation by 2046. The data also showed more hot days in future decades and erractic rainfall pattern by 2046 in both environments. The Genetic Algorithm (GA) appeared to be a good approach to assess climate change impact on pearl millet yield in Punjab, Pakistan, predicting negative yield impacts (11–12%) due to future warming. We suggest broadening tests of this method to other cases around the world, with similar climate regimes.

1. Introduction

Weather and climate are critical abiotic determining factors (important cultural factors include management, technology, institutional contexts, economics etc.) of the success and failure of crops regardless of the type of crop and location (Ullah et al., 2017).

Long-term climate trends are quantifiable (i.e. mean, extreme, and variability in temperature and rainfall) by numerous diagnostic and mathematical methods (IPCC, 2014; Korres et al., 2016; Wang et al., 2016; Li et al., 2018). The worldwide trend toward increasing extreme mean temperatures is obvious (Field et al., 2012; Rezaei et al., 2015) and certain to cause negative impacts on agricultural production systems (crops, forests, livestock, and fisheries) (Ahmad et al., 2015; Ullah et al., 2017).

Daily mean temperature is considered for index of assessment of climate change in most of the cases, but it cannot fully depict the complex impacts of temperature variation on production systems (e.g. non-linear effects or disproportionate impacts of nighttime temperatures) (Alexander et al., 2006; Qu et al., 2014; Dong et al., 2018). Changes in mean air temperature can be driven by changes to either T_{max}, T_{min}, or both (Sun et al., 2006), which result in change in diurnal temperature range ($DTR = T_{max} - T_{min}$). Though the DTR metric has received limited attention in studies of climate change, decreasing global trends in DTR are seen from 1950 to 1990, driven by increases in daily mean temperature and a steady increase in daily maximum temperature (Karl et al., 1991; Qu et al., 2014; Lobell, 2007). Many other factors such as land use and land cover changes (Karl et al., 2004; Riahi et al., 2007), irrigation (Karl et al., 1988), desertification, urbanization (Wang et al., 2012) and other climatic variables (Karl et al., 1993) can affect diurnal air temperature range (DTR). As a result of its integrative

* Corresponding author.
E-mail address: aumalik.aari@gmail.com (A. Ullah).

https://doi.org/10.1016/j.ecolind.2018.03.053
Received 7 July 2017; Received in revised form 26 January 2018; Accepted 22 March 2018
Available online 05 April 2018
1470-160X/ Published by Elsevier Ltd.

nature, the relationship between DTR and crop yield may be interesting in the context of climate change and adaptations studies. For example, an increase in DTR for a given T_{mean} may accurately predict yield reductions due to the increase in water stress and reduction in photosynthesis associated with increased T_{max} (Dhakhwa and Campbell, 1998).

Even short episodes of high temperature, especially when associated with uneven distribution of rainfall, have been shown empirically to have negative effects on crop productivity (Lobell and Field, 2011; Ruane et al., 2015). These changes in weather and climate are likely to exacerbate food insecurity, especially in developing countries (FAO, 2008; Lobell, 2008; Misra, 2014).

Warming of climate systems results in changes in the frequency and intensity of extreme temperature and rainfall events (Coumou and Robinson, 2013). These changes to extreme events can involve shifts in their distribution or changes in the shape of their distributions. Various studies show that a shift in the mean accounts for much the change in observed temperature extremes (Della-Marta et al., 2007; Rhines and Huybers, 2013; McKinnon et al., 2016; Lewis and King, 2016). Both daily maximum (T_{max}) and minimum (T_{min}) temperatures have shifted higher values (over Canada (Bonsal et al. 2001), Africa (Anyah and Qiu, 2012), worldwide (Donat and Alexander, 2012), southern Colorado (Rangwala et al., 2012), and China (Zhang et al., 2017)). Higher temperatures are associated with increased respiration rates, reduction in pollen germination, shorter grain filling period, lower biomass and low yields (Adams et al., 1998). Pre and post flowering heat waves at 35 degree Celsius lead to yield reductions in wheat, barley (*Hordeum vulgare* L. of Grass family), and triticale (Ugarte et al., 2007; Pope, 2012). Consequently, the trend in India towards high yields of wheat, rice, and barley, and low yields in maize and millets is likely to accelerate (Parry, 1990). High temperature above 35 degree Celsius in combination with high humidity and low wind speed caused a 4 degree Celsius increase in temperature, resulting in floret sterility in rice (Tian et al., 2010) and reduce crop yields of maize, soybean, and cotton (Schlenker and Roberts, 2009) and fruit crops (Lobell and Field, 2011).

Changing rainfall patterns over decades has significantly affected crop yields, especially in arid and semi-arid areas like Pakistan. Rainfed crops are particularly vulnerable. Water deficits are associated with a cascade of crop effects including reduced crop biomass, shorter life cycles, lower stem dry weight, reduced leaf area, reduced pollen viability, seed formation problems, and ultimately crop yields (Blum, 1996). Farming communities of Pakistan face serious challenges due to both frequent drought and heat stress. Pakistan is in the top ten most vulnerable countries, with a climate risk index (CRI) value of 31.50, $3.989 billion US loss and 141 extreme events in 1994–2013 (Kreft et al., 2014).

In this context, understanding the baseline historical weather and climate variability that affects agricultural production systems is of significant value for regions like Pakistan. Scientists are using GCMs (General Circulation Models) and artificial intelligence methods such as Genetic Algorithm (GA) to investigate crop yields under future projected climate scenarios. We utilize this approach to explore of the impacts of expected changes in temperature and rainfall extremes on millet in Punjab, Pakistan. We analyze historical (1980–2010) and mid-century (2046) projections in decades for two contrasting environments of Punjab, Pakistan using statistical indices (RMSE, Pearson, Spearman, MAE, NSE and d) from model simulation output files. We further applied GA to estimate weather and climate extreme indicators and pearl millet yield for three future decades.

2. Materials and methods

2.1. Study area

This study area (Fig. 1) was comprised of two different locations on the basis of climatic conditions: the Layyah district (arid) and the Faisalabad district (semi arid). Faisalabad is located in Punjab province, Pakistan at 31°26′N, 73°04′E (altitude 184 m); Karor Lal Eason (Layyah) is also in Punjab province, Pakistan at 31° 13′N, 70° 58′E (altitude 158 m). The calculated driving distance from Faisalabad to Karor Lal Eason (Layyah) is 242 km.

2.2. Datasets

For observations, two datasets were used and those cover thirty years (1980–2010) long period. The AgMERRA dataset was generated using linear interpolation technique for Karor (Layyah), which was compiled by Pakistan Meteorological Department (PMD), Islamabad by merging data from different sources. Data inputs were derived from MERRA (Modern Era Retrospective-analysis for Research and Applications) and CFSR (Climate Forecast System Reanalysis), to compensate for limited weather observatories. The data were generated as described by Alex et al. (2015) with the following equations used to calculate T_{min}, T_{max} and precipitation.

$$T_{avgAgMERRA}(d,m) = T_{avgMERRA}(d,m) + \overline{T}_{Adj} \quad (1)$$

$$T_{maxAgMERRA}(d,m) = T_{maxMERRA}(d,m) + \overline{T}_{Adj}(m) + \gamma(DTR_{CRU}(\overline{m}) - (DTR_{MERRA}(\overline{m})) \quad (2)$$

$$T_{minAgMERRA}(d,m) = T_{minMERRA}(d,m) + \overline{T}_{Adj}(m) + \gamma(DTR_{CRU}(\overline{m}) - (DTR_{MERRA}(\overline{m})) \quad (3)$$

$$\acute{P}_{AgMERRA}(d.\ m) = P_{MERRAland}(d,m) \times \frac{1}{3}\{(\overline{P}_{MERRAland}(m) + (\overline{P}_{WM}(m) + (\overline{P}_{GPCC}(m)/(\overline{P}_{MERRAland}(m)\} \quad (4)$$

where, $T_{avgAgMERRA\ (d,m)}$ is the average temperature for any given day "d" in month "m". $\overline{T}_{Adj}(m)$ is the difference in average temperatures for any given month. DTR_{CRU} $(\overline{m})$, is the diurnal temperature range taken from Climatic Research Unit (CRU) using days in given month "m" from all years. Similarly, $\acute{P}_{AgMERRA}(d.\ m)$, is the average precipitation for any given day "d" and month "m". $\overline{P}_{GPCC}(m)$, is the precipitation data for given month "m" taken from Global Precipitation Climatology Centre (GPCC). $(\overline{P}_{WM}(m)$means mean precipitation for given month "m" as determined by Willmott and Matsuura, 1995; WM.

Daily T_{min}, T_{max} and T_{avg} were linearly interpolated from available from MERRA and CFSR data. The average temperature for each month (m) was reanalysed as adapted by Harris et al. (2013). The biases were reduced by comparing average monthly values provided by Climatic Research Unit (CRU) TS3.1; Harris et al., 2013) and Willmott and Matsuura, 1995 against the corresponding mean monthly temperature from interpolated reanalysis (Rosenzweig et al., 2013).

The observed dataset for baseline period (1980–2010) was collected from the Crop Physiology Section, Department of Agronomy, University of Agriculture, Faisalabad. MIRCO5 and GFDL-ESM2M simulations models from CMIP5 were used for future Representative Concentration Pathways (RCP) scenarios (RCP4.5 low emissions and RCP8.5 high emissions) to project decadal changes in temperature and rainfall across two selected contrasting environments of Punjab, Pakistan. We selected three decades for future prediction: 2017–2026 (1st decade), 2027–2036 (2nd decade), and 2037–2046 (3rd decade) and compared decadal variabilities with period 2006–2015.

2.3. Efficiency criteria

We used the following four efficiency criteria: Index of agreement "d" (Willmot, 1981); mean absolute error "MAE" (MacLean, 2005); Nash-Sutcliffe efficiency "NSE" (Nash and Sutcliffe, 1970); root mean square error "RMSE" (MacLean, 2005).

The index of agreement "d", represents the ratio of the mean square error and the potential error, calculated via Eq. (5):

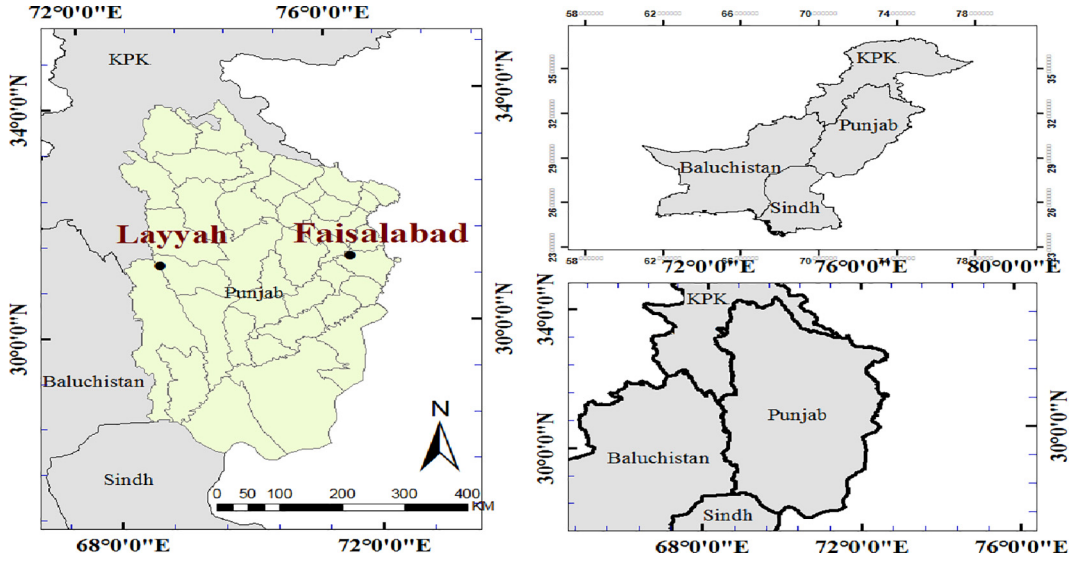

Fig. 1. Geographical location of Faisalabad and Layyah Stations, Punjab, Pakistan.

$$d = 1 - \frac{\sum_{i=1}^{n} (O_i - P_i)^2}{\sum_{i=1}^{n} (|P_i - \overline{O}| + |O_i - \overline{O}|)^2}, \quad 0 \leqslant d \leqslant 1 \tag{5}$$

where O are the observed and P are the predicted values. The range of d lies between 0 (no correlation) and 1 (perfect fit).

Mean absolute error was computed to determine overall magnitude of error. MAE is given by:

$$MAE = \frac{\sum_{i=1}^{N} |P_i - O_i|}{N} \tag{6}$$

where N is the number of samples, P is the predicted weather value, and O is the observed weather data value.

The Nash-Sutcliffe efficiency NSE (1970) is a normalized means of comparing error between observed and predicted values, computed as:

$$NSE = 1 - \frac{\sum_{i=1}^{n} (O_i - P_i)^2}{\sum_{i=1}^{n} (O_i - \overline{O})^2} \tag{7}$$

NSE ranges between 1.0 (perfect fit) and $-\infty$. An efficiency of lower than zero indicates that the mean value of the observed time series would have been a better predictor than the model (Krause et al., 2005).

RMSE measures the average magnitude of error, calculated as the square root of the average of squared differences between prediction and observation data:

$$RMSE = \sqrt{\sum_{i=1}^{n} (O_i - P_i)^2 / n} \tag{8}$$

2.4. Statistical downscaling

The spatial resolution of GCMs is often too coarse (approximately 150 km) for addressing climate change impacts at the local scale (Wetterhall et al., 2012). Therefore, statistical downscaling approaches are generally designed to present fine-scale regional information. Two basic methods are utilized toward this end: the bias correction and spatial downscaling (BCSD) method, and the constructed analogs (CA) method. The BCSD method has been used extensively (Wood et al., 2004; Salathe et al., 2007; Karl et al., 2009). In this study we used Delta method for BCSD (Amengual et al., 2012, Chen et al., 2013; Bennett et al., 2014), calculated as follows (Eqs. (9) and (10)):

$$P_{Pre.} = P_{GCM} \times \frac{\mu(P_{Obs.})}{\mu(P_{GCM})} \tag{9}$$

$$T_{Pre.} = T_{GCM} + \mu(T_{Obs.}) - \mu(T_{GCM}) \tag{10}$$

where P_{GCM} and P_{Obs} are the GCM precipitation data and observed precipitation, respectively; T_{GCM} and T_{Obs} are the GCM temperature data and the observed temperature, respectively; and μ is the mean of data in the period.

2.5. Genetic Algorithm method (GA)

GA is a stochastic search algorithm that begins from an initial random set of solutions called chromosomes, composed of elements called genes. Genetic Algorithms' fitness function assigns a numeric value to a question and is usually the goal for optimization. The process includes: 1-Selection: We used the most common way to select variables – the roulette wheel, 2- Crossover: we used a two-point crossover, 3-Mutation: we performed the mutation using a uniform method. Fitness function in this study for GA were determined according to Eq. (11). The aim of GA is to achieve the minimum value for the fitness function.

$$\text{Fitness} = \text{Minimize}\left\{\sum_{i=1}^{31} |(Y_i^{obs} - Y_i^{sim})|\right\} \tag{11}$$

where Y_i^{obs} is the yield of the observation period and Y_i^{sim} is the yield of the simulation period. For predicting yield of millet we calculated regression coefficient via the GA method, using equation 11 for obtaining yield prediction, and Eq. (12) with the effective months for millet from Jun to November.

$$Y_{year} = \left(\sum_{m=6}^{12} a_m \times P_{m,year}\right) + \left(\sum_{m=6}^{12} b_m \times DTR_{m,year}\right) \tag{12}$$

In Eq. (8) m in a_m and b_m are the coefficients from 6 to 12 from 6 months for precipitation and DTR, respectively. $P_{m,\ year}$ is the value of precipitation for month m and applicable year. The $DTR_{m,\ year}$ refers to the value of DTR for month (m) and applicable year. Each chromosome consists of 12 genes that include coefficients of a and b in Eq. (12) (Table 1). The proper coefficients are obtained when the fitness as determined by Eq. (11) is minimized.

Table 1
Coefficients of regression equation for prediction yield.

Chromosome											
a1	a2	a3	a4	a5	a6	b1	b2	b3	b4	b5	b6
Gene1, …											Gene12

Table 2
Efficiency criteria results for evaluation of predicted (GCMs) and observed data (AgMERRA) for 2006–2010 in Faisalabad and Layyah, Pakistan.

	Data	d	MAE	NSE	RMSE
Faisalabad	Tmin	0.98	1.9	0.93	3.9
	Tmax	0.95	2.8	0.87	5.4
	Precipitation	0.67	52	0.2	9
Layyah	Tmin	0.98	2	0.92	3.7
	Tmax	0.95	4	0.8	6.5
	Precipitation	0.45	45.7	0.1	8.2

3. Results and discussion

3.1. Model accuracy evaluation

The efficiency criteria calculated for observed (AgMERRA dataset) and predicted values (GCMs) for the common period (2006–2010) are presented in Table 2. A perfect model returns a value of 1 for NSE, indicating simulated values exactly match the observed values. As seen in Table 2, modeled T_{min} and T_{max} have NSE values very close to 1 for both locations. Modeled precipitation is not strong as efficient due to erratic precipitation patterns at both locations (Table 2).

3.2. Observed data and future projections

The Taylor diagrams of the Faisalabad location data (Fig. 2) show good correlation (0.90–0.99) between observed and projected T_{max} and T_{min} in both models, with consistently lower correlations for precipitation. Overall, MIROC5 with the Delta method had the best performance under RCP4.5 for T_{min} prediction with correlation of 0.98 and RMSE of 1.1. The MIROC5 model under RCP 8.5 performed the best for T_{max}. For precipitation, GFDL under RCP8.5 returned the best correlation value at 0.50.

For the Layyah location (Fig. 3), MIRCO5 was the best model (correlation of 0.92) for T_{min} prediction under RCP4.5. T_{max} was best modeled (correlation of 0.97) with MIROC5 under RCP 8.5. GFDL predicted precipitation well under RCP8.5.

T_{min} at Layyah monthly trends varied under the MIROC5 under RCP4.5 projections. For the CMPI5 model, the baseline period (2006–2015) and the first future decade (2017–2026) showed similar patterns, with the exceptions of March and October, which show a 1 degree Celsius increase in Minimum Mean Monthly T_{min} (MT_{min}). The second future decade (2027–2036) has greater changes, showing increases of MT_{min} for January, April, June, September and November, by 1.5, 2, 2.5, 0.75 and 1 °C, respectively relative to the baseline period. The greatest changes in MT_{min} relative to baseline for the third future decade (2037–2046) were predicted for January, October and November, with values of 1.9, 1.5 and 1.5 °C, respectively. MT_{min} for Faisalabad station is expected to increase in the future under RCP4.5, with an increase of around 2 °C expected in June during 2027–2036 and 2037–2046 and an increase of around 2.5 °C in September in 2026–2035 (Fig. 4).

March has the greatest projected changes in both stations' Maximum Mean Monthly T_{max} (MT_{max}), with an increase of 3.3 °C for Layyah and 3.5 °C for Faisalabad relative to baseline (Fig. 5). Changes at Faisalabad are highest for the 2037–2046 period; however, Layyah

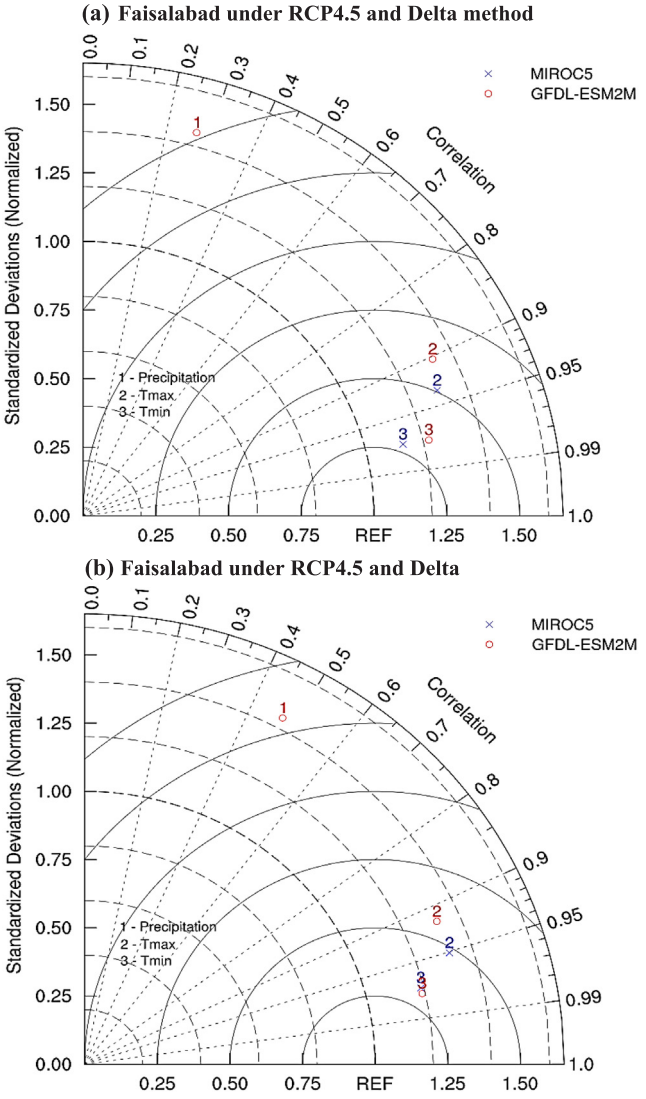

Fig. 2. Taylor diagram of Faisalabad station with two models, under RCP4.5 and RCP8.5 with Delta method for precipitation, Tmax and Tmin for evaluation period, (a) Represents outputs of 2 models under RCP4.5, (b) Represents outputs of two models under RCP8.5.

station shows the greatest impact for 2027–2036 (Fig. 4). At the end of winter, summer and fall, the value of MT_{max} will be increased in 3 decades as compare to 2006–2015 in Layyah and Faisalabad.

The GFDL model projects increases in precipitation in Layyah for Jan., Feb., Apr., Jun., Jul., and Sep., relative to baseline. Increases of more than 50 cm for September are predicted under RCP8.5 for 2036–2045 (Fig. 6). However, the average monthly total precipitation is expected to decrease during the months of March, August, October, and November by at least 2 cm over 2017–2026, 2027–2036, and 2037–2046. A similar trend was observed at Faisalabad, where Precipitation is projected to increase in the future for January, February, April, June, July and September when compare to 2006–2015 (Fig. 6).

The diurnal temperature range (DTR) is predicted to dramatically increase in future decades (2017–2027, 2028–2036, and 2037–2046) compared to observed baseline data (1980–2010) (Fig. 7).

3.3. Prediction of millet yield with GA

The coefficients of the equations for precipitation and DTR were calculated using the GA method and applied to the future projection periods (2017–2026, 2027–2036, and 2037–2046). The resultant

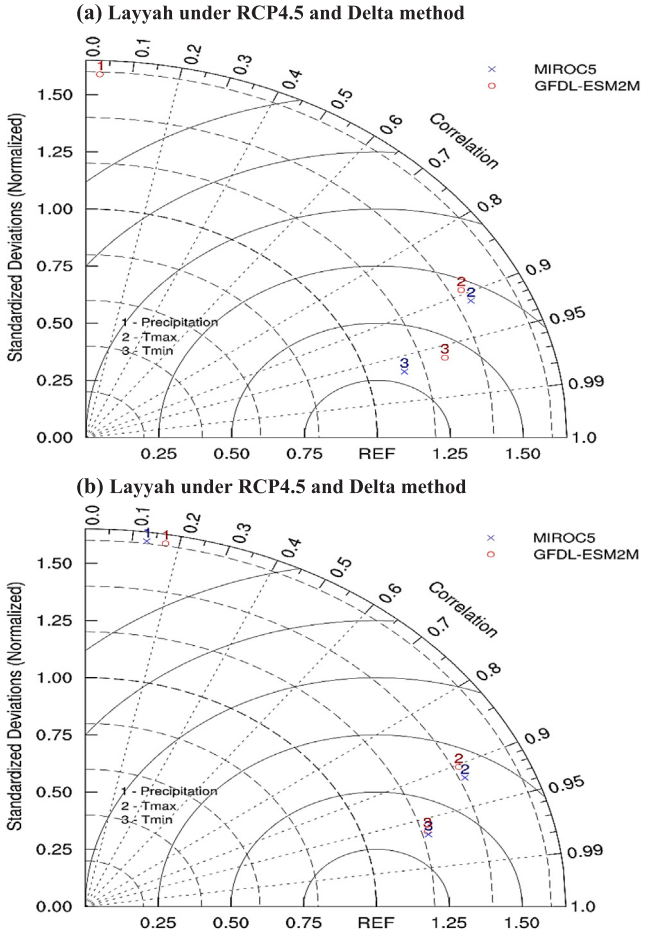

Fig. 3. Taylor diagram of Faisalabad station with two models, under RCP4.5 and RCP8.5 with Delta method for precipitation, T_{max} and T_{min} for evaluation period, (a) Represents outputs of two models under RCP4.5, (b) Represents outputs of two models under RCP8.5.

outputs showed significant regression coefficients between observed yield and simulation yield (Table 3).

From the given results, it can be discussed that increase in extreme precipitation are expected to trigger floods, and the associated impacts will cause probable loss of life and economic damage affecting agricultural production systems (Wu et al., 2015). There are number of ways to assess the loss caused by the dramatic change in temperature and precipitation. The changes in diurnal temperature range is an important aspect to study in association with change in mean temperature (see Table 4.).

Heat waves often cause severe damage to cereal crops (Ugarte et al., 2007; Lobel, 2007; Pope, 2012), but variability in climate is often more detrimental to crops than directional climate change. Dramatic changes in daily temperatures (T_{max}, T_{min}, T_{mean}, DTR) and erratic rainfall events damage crops and create food insecurity. Characterizing these future expected changes in climate allows the development of management adaptations that may mitigate these impacts. Introducing more resilient varieties and crops like pearl millet in high climate risk index countries will surely be part of reasonable adaptation policy (Ullah et al., 2017).

The GA technique based on regression coefficients clearly showed a response of millet yield to increased mean temperature (T_{mean}). In Fig. 8, the observed and simulated of millet yield was presented. In our study GA determined that the negative response of millet yield was observed due to DTR. We forecast a ~12% reduction in yield for future relative to baseline in Punjab, Pakistan.

Our results are in agreement with many processed based model

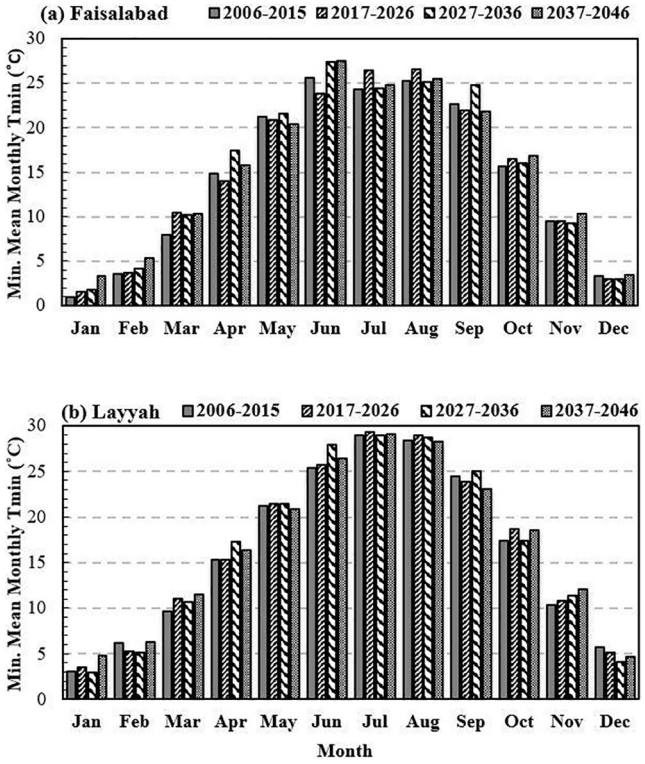

Fig. 4. Minimum mean monthly T_{min} (MT_{min}) projections with MIROC5 under RCP4.5 for (a) Faisalabad, and (b) Layyah.

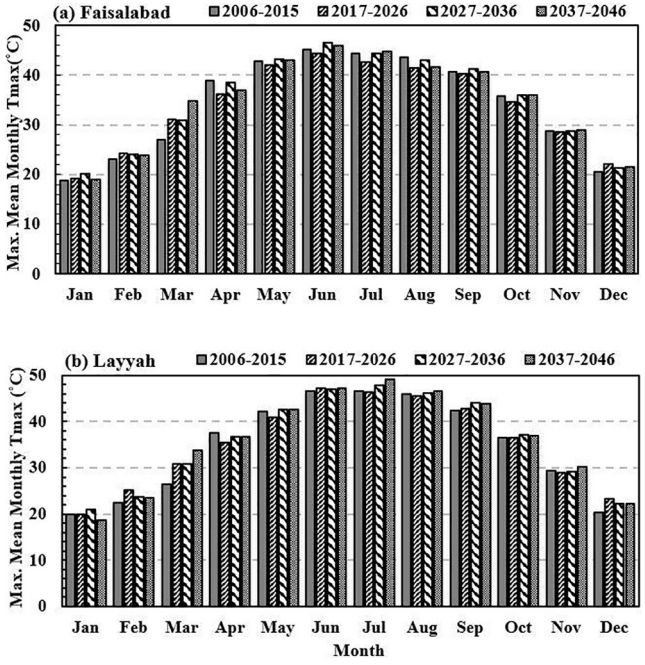

Fig. 5. Maximum mean monthly of T_{max} (MT_{max}) projections with MIROC5 under RCP8.5 for (a) Faisalabad, and (b) Layyah.

outputs that show negative yield response at both small and large scale across different crops (e.g. Rosenzweig and Parry, 1994; Lobell, 2008). Nicholls (1997) reported declining wheat yield associated with DTR changes in Australia. Similarly, Lobell and Ortiz-Monasterio (2007) clarified the positive relationship of DTR with yields due to linkage of high DTR with more values for solar radiation for wheat crop. These negative responses of yield to DTR and T_{mean} showed more harm from increased day time temperatures than from night time temperatures.

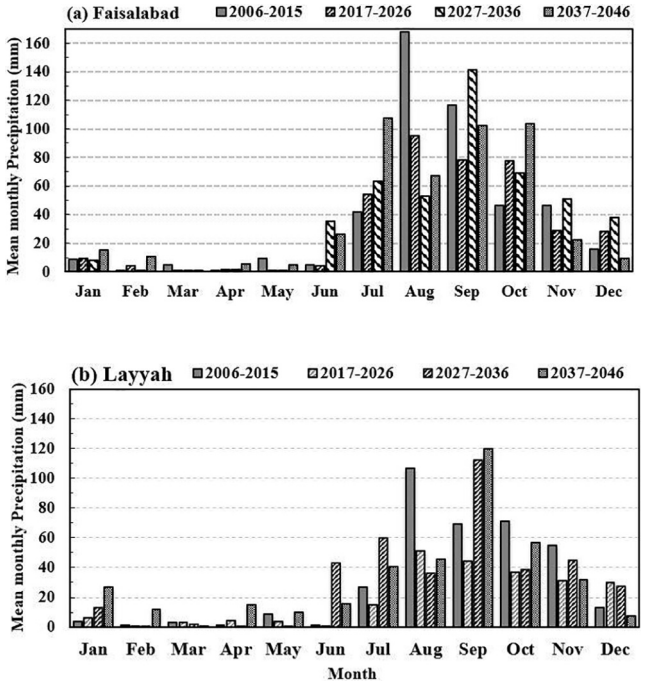

Fig. 6. Monthly mean of precipitation projections with GFDL under RCP8.5 for (a) Faisalabad and (b) Layyah.

Dhakhwa and Campbell (1998) showed a decrease in corn yield with increased DTR using the EPIC crop simulation model. The findings of Tao et al. (2006) were also consistent with our finding that increasing DTR can reduce yields.

Lobell (2007) evaluated inter-annual weather changes in the form of diurnal temperature range (DTR) and assessed national cereal yields. Mean yields were decreased up to 12% with DTR for most of the cereals. However, the clear evidences for millet yield response and DTR relations are not conveyed through GA (Park and Joh, 2005).

This paper presents predictions of important climate change indicators (T_{min}, T_{max}, T_{mean}, DTR, and precipitation) for arid and semi-arid regions of Pakistan using two source datasets, with future trends calculated over three future decades using updated model simulations from CMIP5 and the RCP4.5 and 8.5 emissions scenarios. Importantly, the simulated and observed indices are calculated using similar approach. We show stronger negative yield effects in arid environment (Layyah) than in semi-arid conditions (Faisalabad), which represent > 12.5% and > 17.5% of world cover, respectively (Sillmann et al., 2013). Several studies focused on the common errors and/or

Table 3
Statistics test for two stations between observed and simulated millet grain yield.

Location	R square	P-Value
Faisalabad	0.62	0.01*
Layyah	0.52	0.01*

Table 4
Average predicted yield (tones ha^{-1}) of pearl millet for three future decades.

Decades	Predicted Yield (tones ha^{-1})	
	Faisalabad	Layyah
2017–2026	1.19	0.98
2027–2036	1.22	1.30
2037–2046	1.25	1.26

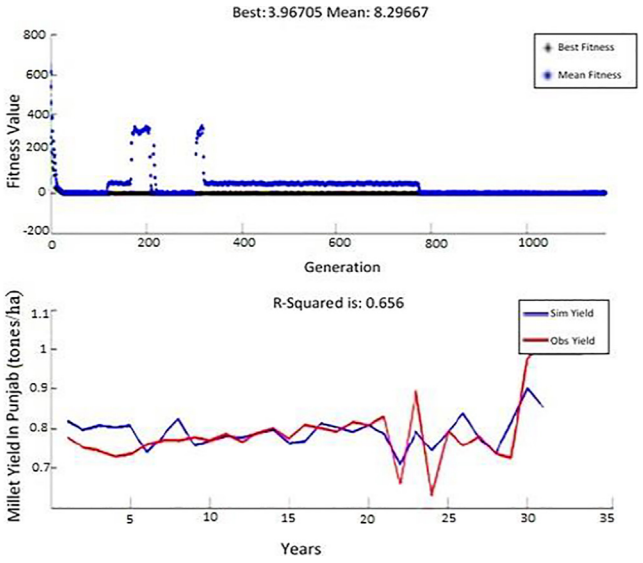

Fig. 8. Assessment of impacts on pearl millet yield via Genetic Algorithm for fitness value; Comparison between observed and simulated yield.

frequency and intensity of daily precipitation simulations of different climate models (Dai et al., 1999; Sun et al., 2007; Brown et al., 2010). Our assessment of two models showed good agreement between the observed and predicted precipitation (Table 2).

MIROC5 future projections show increasing average temperatures and increasing likelihood of extreme heat events in the arid and semi-

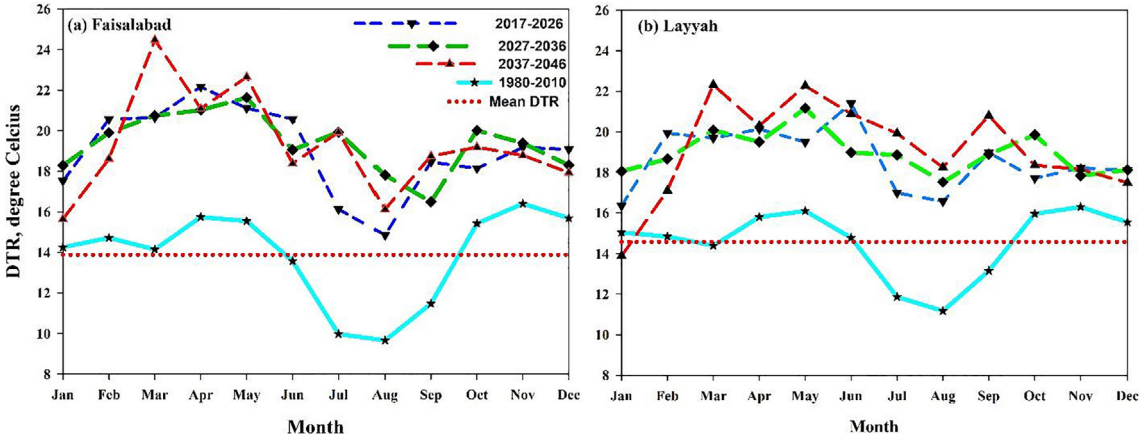

Fig. 7. Mean monthly DTR values of (a) Faisalabad and (b) Layyah Station in base period (1980–2010) and future three decades.

arid environments of Punjab Pakistan. This highlights a significant challenge for future decades (up to 2046, or mid-century): mitigation of the severity of future extreme heat events' impacts on agriculture. These changes appear to scale with the intensity of emissions scenarios (RCP4.5 and RCP8.5). The projected changes in precipitation extremes are more consistent using the GFDL model, with both moisture environments showing robust changes at the mid-century time scale (King et al., 2015; Gibson et al., 2017).

4. Conclusions

Predicted climate warming can result in changes to average temperatures, changes the frequency of extreme temperature events, and erratic rainfall patterns. Changes in mean air temperature are reflected in the diurnal temperature range (DTR) metric, which can be altered due to changes in T_{max}, T_{min}, or a combination of both. This important index has received limited attention in studies of climate change. We observed a decreasing trend in DTR from 2017 to 2046, due to increases in daily mean temperature and a steady increase in daily maximum temperature. Increasing DTR for a given T_{mean} may cause in reduction of yield, because the related increase in T_{max} causes increase in water stress and reduction in photosynthesis rate. The algorithm output showed significant decreases in yield in future due to decadal climate variability. Introducing the most resilient crops like pearl millet in high climate risk index countries like Pakistan is a reasonable approach to mitigate the expected changes in weather and climate. Our core findings are:

- MIROC5 is useful climate model and performed well for our regions of interest; (Faisalabad (semi-arid) and Layyah (arid) district of Punjab, Pakistan), with strong correlation (0.90–0.99) between observed and projected T_{max} and T_{min}; GFDL was a better predictor of precipitation than MIROC5.
- First decade in future (2017–2026) showed less changes except the changes in March (increase of 3.3 °C for Layyah and 3.5 °C for Faisalabad) and October with 1 °C increase in temperature relative to baseline, for future. The second decade (2027–2036) showed the highest values of changes with increasing trend of Tmin (e-g for January, April, June, September and November with values of 1.5, 2, 2.5, 0.75 and 1 °C, respectively). The most changes in 3rd decade (2037–2046) were observed during the month of January, October and November. Tmin has the highest variations in compare to base period, with values of 1.9, 1.5 and 1.5 °C, respectively. These variabilities are expected to occur in the end of winter, summer and fall seasons at both locations.
- The GFDL climate model predicted decrease in cumulative monthly precipitation during the month of March, August, October and November (by at least 20 mm) over all future three decades (2017–2046) at both locations.
- Genetic Algorithm (GA) approach was useful in predicting yield pearl millet under future changing climate scenarios in Punjab, Pakistan. This approach quantified decrease in millet grain yield up to 12% in Punjab, Pakistan and need to develop suitable adaptation strategies to overcome impact of climate variability on millet and other cereals.

Acknowledgements

We would like to thank K. Grace Crummer (Institute for Sustainable Food Systems, University of Florida, USA) for editing the English used in the manuscript. This work would not be possible without the International Research Support Initiative Programme (IRSIP) scholarship awarded by the Higher Education Commission, Islamabad-Pakistan to first author for his visit to the Institute for Sustainable Food Systems, University of Florida, USA. Thanks to Prof. Dr. Gerrit Hoogenboom, University of Florida, USA for his guidance and technical support during the entire period of Dr. Asmat Ullah's stay in USA.

References

Adams, R.M., Hurd, B.H., Lenhart, S., Leary, N., 1998. Effects of global climate change on agriculture: an interpretative review. Clim. Res. 11, 19–30. http://dx.doi.org/10.3354/cr011019.

Ahmad, A., Ashfaq, M., Rasul, G., Wajid, S.A., Khaliq, T., Rasul, F., Saeed, U., Habib-ur-Rahman, M., Hussain, J., Baig, I.A., Naqvi, S.A.A., Bokhari, S.A.A., Ahmad, S., Naseem, W., Hoogenboom, G., Valdivia, R.O., 2015. Impact of climate change on the rice-wheat cropping system of Pakistan. In: Rosenzweig, Cynthia, Hillel, Daniel (Eds.), The agricultural model inter-comparison and improvement project (AgMIP) integrated crop and economic assessments, Part 2. ICP series on climate change impact, adaptation, and mitigation. Joint Publication with American Society of Agronomy, Crop Science Society of America, and Soil Science Society of America, Imperial College Press, pp. 219–258.

Alex, C.R., Goldberg, R., Chryssanthacopoulos, J., 2015. Climate forcing datasets for agricultural modelling: merged products for gap filling and historical climate series estimation. Agric. For. Meteorol. 200, 233–248.

Alexander, L.V., Zhang, X., Peterson, T.C., Caesar, J., Gleason, B., et al., 2006. Global observed changes in daily climate extremes of temperature and precipitation. J. Geophys. Res. 111 (D5), D05109. http://dx.doi.org/10.1029/2005JD006290.

Amengual, A., Homar, V., Romero, R., Alonso, S., Ramis, C., 2012. A statistical adjustment of regional climate model outputs to local scales: application to Platja de Palma, Spain. Am. Meteorol. Soc. 939–957. http://dx.doi.org/10.1175/JCLI-D-10-05024.1.

Anyah, R.O., Qiu, W., 2012. Characteristic 20th and 21st century precipitation and temperature patterns and changes over the Greater Horn of Africa. Int. J. Climatol. 32, 347–363. http://dx.doi.org/10.1002/joc.2270.

Bennett, C., Grose, R., Corney, P., White, J., Holz, K., Katzfey, J., Post, A., Bindoff, L., 2014. Performance of an empirical bias-correction of a high-resolution climate dataset. Int. J. Climatol. 34, 2189–2204. http://dx.doi.org/10.1002/joc.3830.

Blum, A., 1996. Crop responses to drought and the interpretation of adaptation. Plant Growth Regul. 20, 135–148. http://dx.doi.org/10.1007/BF00024010.

Bonsal, B.R., Zhang, X., Vincent, L.A., Hogg, W.D., 2001. Characteristics of daily and extreme temperatures over Canada. J. Clim. 14, 1959–1976. http://dx.doi.org/10.1175/1520-0442(2001) 014<1959:CODAET>2.0.CO;2.

Brown, J.R., Jakob, C., Haynes, J.M., 2010. An evaluation of rainfall frequency and intensity over the Australian region in a global climate model. J. Clim. 23, 6504–6525. http://dx.doi.org/10.1175/2010JCLI3571.1.

Chen, J., Brissette, F.P., Chaumont, D., Braun, M., 2013. Performance and uncertainty evaluation of empirical downscaling methods in quantifying the climate change impacts on hydrology over two North American river basins. J. Hydrol. 479, 200–214. http://dx.doi.org/10.1016/j.jhydrol.2012.11.062.

Coumou, D., Robinson, A., 2013. Historic and future increase in the global land area affected by monthly heat extremes. Environ. Res. Lett. 8 (3), 034018. http://dx.doi.org/10.1088/1748-9326/8/3/034018.

Dai, A., Trenberth, K.E., Karl, T.E., 1999. Effects of clouds, soil moisture, precipitation, and water vapor on diurnal temperature range. J. Clim. 12, 2451–2473.

Della-Marta, P.M., Haylock, M.R., Luterbacher, J., Wanner, H., 2007. Doubled length of western European summer heat waves since 1880. J. Geophys. Res. Atm. 112 (D15), D15103–D15111. http://dx.doi.org/10.1029/2007JD008510.

Dhakhwa, G.B., Campbell, C.L., 1998. Potential effects of differential day-night warming in global climate change on crop production. Clim. Change 40, 647–667.

Donat, M.G., Alexander, L.V., 2012. The shifting probability distribution of global daytime and night-time temperatures. Geophys. Res. Lett. 39 (14), L14707. http://dx.doi.org/10.1029/2012GL052459.

Dong, Z., Pan, Z., He, Q., et al., 2018. Vulnerability assessment of spring wheat production to climate change in the Inner Mongolia region of China. Ecol. Indic. 85, 67–78. http://dx.doi.org/10.1016/j.ecolind.2017.10.008.

FAO, 2008. Climate Change and Food Security: A Framework Document. FAO, Rome, Italy.

Field, C.B., Barros, V., Stocker, T.F., Dahe, Q., 2012. Managing the Risks of Extreme Events and Disasters to Advance Climate Change Adaptation: Special Report of the Intergovernmental Panel on Climate Change. Cambridge University Press.

Gibson, P., Perkins-Kirkpatrick, S.E., Alexander, L.V., Fischer, E.M., 2017. Comparing Australian heatwaves in the CMIP5 models through cluster analysis. J. Geophys. Res. Atmos. 122 (6), 3266–3281. http://dx.doi.org/10.1002/2016JD025878.

Harris, I., Jones, P.D., Osborn, T.J., Lister, D.H., 2013. Updated high-resolution grids of monthly climatic observations—the CRU TS3.10 dataset. Int. J. Climatol. http://dx.doi.org/10.1002/joc.3711.

IPCC, 2014. Climate change 2014: impacts, adaptation, and vulnerability. Part A: global and sectoral aspects. In: Field, C.B., Barros, V.R., Dokken, D.J. (Eds.), Contribution of Working Group II to the Fifth Assessment Report of the Intergovernmental Panel on Climate Change. Cambridge University Press, , Cambridge, United Kingdom and New York. NY, USA 1132 p.

Karl, B., Karoly, D.J., Arblaster, J.M., 2004. Diurnal temperature range as an index of global climate change during the twentieth century. Geophys. Res. Lett. 31, L13217. http://dx.doi.org/10.1029/2004GL019998.

Karl, T.R., Diaz, H.F., Kukla, G., 1988. Urbanization: its detection and effect in the United States climate record. J. Clim. 1 (11), 1099–1123. http://dx.doi.org/10.1175/1520-0442(1988) 001<1099:UIDAEI>2.0.CO;2.

Karl, T.R., Knight, R.W., Gallo, K.P., Peterson, T.C., Jones, P.D., Kukla, G., Plummer, N., Razuvayev, V., Lindseay, J., Charlson, R.J., 1993. A new perspective on recent global warming: asymmetric trends of daily maximum and minimum temperature. Bull. Am. Meteorol. Soc. 74, 1007–1023. http://dx.doi.org/10.1175/1520-0477(1993)

074 < 1007:ANPORG > 2.0.CO;2.
Karl, T.R., Kukla, G., Razuvayev, V.N., 1991. Global warming: evidence for asymmetric diurnal temperature change. Geophys. Res. Lett. 18, 2253–2256.
Karl, T.R., Melillo, J.M., Peterson, T.C., Hassol, S.J., 2009. Global Climate Change Impacts in the United States. Cambridge University Press, New York.
King, A.D., Donat, M.G., Alexander, L.V., Karoly, D.J., 2015. The ENSO-Australian rainfall teleconnection in reanalysis and CMIP5. Clim. Dyn. 44 (9–10), 2623–2635. http://dx.doi.org/10.1007/s00382-014-2159-8.
Korres, N.E., Norsworthy, J.K., Tehranchian, P., Gitsopoulos, T.K., Loka, D.A., Oosterhuis, D.M., Gealy, D.R., Moss, S.R., Burgos, N.R., Miller, M.R., Palhano, M., 2016. Cultivars to face climate change effects on crops and weeds: a review. Agron. Sustainable Dev. 36 (12), 2–22. http://dx.doi.org/10.1007/s13593-016-0350-5.
Krause, P., Boyle, D.P., Base, F., 2005. Comparison of different efficiency criteria for hydrological model assessment. Adv. Geosci. 5, 89–97. http://dx.doi.org/10.5194/adgeo-5-89-2005.
Kreft, S.D., Eckstein, L., Junghans, L., Kerestan, C., Hagen, U., 2014. Global Climate Risk Index 2015. German watch e.V. Office Bonn. 2–6. ISBN: 978-3-943704-23-5
Lewis, S.C., King, A., 2016. Evolution of mean, variance and extremes in 21st century temperatures. Weather Clim. Extremes 15, 1–10. http://dx.doi.org/10.1016/j.wace.2016.11.002.
Li, F., Xu, Z., Ma, H., 2018. Can China achieve its CO_2 emissions peak by 2030? Ecol. Indic. 84, 337–344. http://dx.doi.org/10.1016/j.ecolind.2017.08.048.
Lobell, D.B., 2007. Changes in diurnal temperature range and national cereal yields. Agric. For. Meteorol. 145, 229–238. http://dx.doi.org/10.1016/j.agrformet.2007.05.002.
Lobell, D.B., 2008. Prioritizing climate change adaptation needs for food security in 2030. Science 319, 607–610. http://dx.doi.org/10.1126/science.1152339.
Lobell, D.B., Field, C.B., 2011. California perennial crops in a changing climate. Clim. Change 109 (1), 317–333. http://dx.doi.org/10.1007/s10584-011-0303-6.
MacLean, A., 2005. Statistical Evaluation of WATFLOOD (Ms). University of Waterloo, Ontario, Canada.
McKinnon, K.A., Rhines, A., Tingley, T.P., Huybers, P., 2016. The changing shape of Northern hemisphere summer temperature distributions. J. Geophys. Res. Atm. 121 (15), 8849–8868. http://dx.doi.org/10.1002/2016JD025292.
Misra, A.K., 2014. Climate change and challenges of water and food security. Int. J. Sustainable Built Environ. 3 (1), 153–165. http://dx.doi.org/10.1016/j.ijsbe.2014.04.006.
Nash, J.E., Sutcliffe, J.V., 1970. River flow forecasting through conceptual models, Part I – a discussion of principles. J. Hydrol. 10 (3), 282–290. http://dx.doi.org/10.1016/0022-1694(70)90255-6.
Nicholls, N., 1997. Increased Australian wheat yield due to recent climate trends. Nature 387, 484–485.
Park, H.S., Joh, M., 2005. Climate change due to the gradual increase in atmospheric CO_2: a climate system model sensitivity study. Key. Eng. Mater. 277–279, 595–600.
Parry, M.L., 1990. Climate Change and World Agriculture. Earth Scan Publications, London.
Pope, K.S., 2012. Climate change adaptation: temperate perennial crops, presented at the California Department of Food and Agriculture. Climate Change Adaptation Consortium, November 28, Modesto, CA.
Qu, M., Wan, J., Hao, X., 2014. Analysis of diurnal air temperature range in the continental United States. Weather Clim. Extremes 4, 86–95. http://dx.doi.org/10.1016/j.wace.2014.05.002.
Rangwala, I., Barsugli, J., Cozzetto, K., Neff, J., Prairie, J., 2012. Mid-21st century projections in temperature extremes in the southern Colorado Rocky Mountains from regional climate models. Clim. Dyn. 39 (7–8), 1823–1840. http://dx.doi.org/10.1007/s00382-011-1282-z.
Rezaei, E.E., Webber, H., Gaiser, T., Naab, J., Ewert, F., 2015. Heat stress in cereals; mechanism and modeling. Eur. J. Agron. 64, 98–113. http://dx.doi.org/10.1016/j.eja.2014.10.003.
Rhines, A., Huybers, P., 2013. Frequent summer temperature extremes reflect changes in the mean, not the variance. Proc. Natl. Acad. Sci. 110 (7). http://dx.doi.org/10.1073/pnas.1218748110.
Riahi, K., Gruebler, A., Nakicenovic, N., 2007. Scenarios of long-term socio-economic and environmental development under climate stabilization. Technol. Forecast Soc. Change 74 (7), 887–935 (Special Issue: Greenhouse Gases – Integrated Assessment).
Rosenzweig, C., Parry, M.L., 1994. Potential impact of climate-change on world food-supply. Nature 367, 133–138.
Rosenzweig, C., et al., 2013. The Agricultural Model Intercomparison and Improvement Project (AgMIP): protocols and pilot studies. Agric. Forest Meteorol. 170, 166–182. http://dx.doi.org/10.1016/j.agrformet.2012.09.011.
Ruane, A.C., Goldberg, R., Chryssanthacopoulos, J., 2015. Climate forcing datasets for agricultural modelling: merged products for gap filling and historical climate series estimation. Agric. For. Meteorol. 200, 233–248. http://dx.doi.org/10.1016/j.agrformet.2014.09.016.
Salathe, E.P., Mote, P.W., Wiley, M.W., 2007. Review of scenario selection and downscaling methods for the assessment of climate change impacts on hydrology in the United States Pacific Northwest. Int. J. Climatol. 27 (12), 1611–1621. http://dx.doi.org/10.1002/joc.1540.
Schlenker, W., Roberts, M.J., 2009. Nonlinear temperature effects indicate severe damages to U.S. crop yields under climate change. PNAS 106 (37), 15594–15598. http://dx.doi.org/10.1073/pnas.0906865106.
Sillmann, J., Kharin, V.V., Zhang, X., Zwiers, F.W., Bronaugh, D., 2013. Climate extremes indices in the CMIP5 multi-model ensemble: Part 1. Model evaluation in the present climate. J. Geophys. Res. Atmos. 118, 1716–1733. http://dx.doi.org/10.1002/jgrd.50203.
Sun, D., Pinker, R., Kafatos, M., 2006. Diurnal temperature range over the United States: a satellite view. Geophys. Res. Lett. 33 (5), L05705. http://dx.doi.org/10.1029/2005GL024780.
Sun, Y., Solomon, S., Dai, A., Portmann, R.W., 2007. How often will it rain? J. Clim. 20 (19), 4801–4818. http://dx.doi.org/10.1175/JCLI4263.1.
Tao, F., Yokozawa, M., Xu, Y., Hayashi, Y., Zhang, Z., 2006. Climate changes and trends in phenology and yields of field crops in China, 1981–2000. Agric. For. Meteorol. 138, 82–92.
Tian, X., Matsui, T., Li, S., Yoshimoto, M., Kobayasi, K., Hasegawa, T., 2010. Heat-induced floret sterility of hybrid rice (Oryza sativa) cultivars under humid and low wind conditions in the field of Jianghan Basin, China. Plant Prod. Sci. 13 (3), 243–251. http://dx.doi.org/10.1626/pps.13.243.
Ugarte, C., Calderini, D.F., Slafer, G.A., 2007. Grain weight and grain number responsiveness to preanthesis temperature in wheat, barley and triticale. Field Crop Res. 100 (2), 240–248. http://dx.doi.org/10.1016/j.fcr.2006.07.010.
Ullah, A., Ahmad, A., Khaliq, T., Akhtar, J., 2017. Recognizing production options for pearl millet in Pakistan under changing climate scenarios. J. Integr. Agric. 16 (4), 762–773. http://dx.doi.org/10.1016/S2095-3119(16)61450-8.
Wang, K., Ye, H., Chen, F., Xiong, Y., Wang, C., 2012. Urbanization effect on the diurnal temperature range: different roles under solar dimming and brightening. J. Clim. 25, 1022–1027. http://dx.doi.org/10.1175/JCLI-D-10-05030.1.
Wang, S., Zhou, C., Li, G., Feng, K., 2016. CO_2, economic growth, and energy consumption in China's provinces: investigating the spatiotemporal and econometric characteristics of China's CO_2 emissions. Ecol. Indic. 69, 184–195. http://dx.doi.org/10.1016/j.ecolind.201604.022.
Wetterhall, F., Pappenberger, F., He, Y., Freer, J., Cloke, H.L., 2012. Conditioning model output statistics of regional climate model precipitation on circulation patterns. Nonlin. Processes Geophys. 19, 623–633. http://dx.doi.org/10.5194/npg-19-623-2012.
Willmot, C.J., 1981. On the validation of models. Phys. Geogr. 2, 184–194.
Willmott, C.J., Matsuura, K., 1995. Smart interpolation of annually averaged air temperature in the United States. J. Appl. Meteorol. 34 (12), 2577–2586.
Wood, A.W., Leung, L.R., Sridhar, V., Littermate, D.P., 2004. Hydrologic implications of dynamical and statistical approaches to downscaling climate model outputs. Clim. Change 62 (1), 189–216. http://dx.doi.org/10.1023/B:CLIM.0000013685.99609.9e.
Wu, C.H., Huang, G.R., Yu, H.J., 2015. Prediction of extreme floods based on CMIP5 climate models: a case study in the Beijing River basin, South China. Hydrol. Earth Syst. Sci. 19, 1385–1399. http://dx.doi.org/10.5194/hess-19-1385-2015.
Zhang, Y., Fu, L., Pan, J., Xu, Y., 2017. Projected changes in temperature extremes in China using PRECIS. Atmosphere 8, 15. http://dx.doi.org/10.3390/atmos8010015.